LBL-16832
Preprint c.2

Lawrence Berkeley Laboratory

UNIVERSITY OF CALIFORNIA

RECEIVED
LAWRENCE
BERKELEY LABORATORY

JAN 17 1984

LIBRARY AND
DOCUMENTS SECTION

Accelerator & Fusion Research Division

Submitted to the Review of Scientific Instruments

ION SOURCE OPERATION WITH DIFFERENT MAGNETIC CONFINEMENT GEOMETRIES

K.N. Leung and K.W. Ehlers

October 1983

TWO-WEEK LOAN COPY

This is a Library Circulating Copy which may be borrowed for two weeks. For a personal retention copy, call Tech. Info. Division, Ext. 6782.

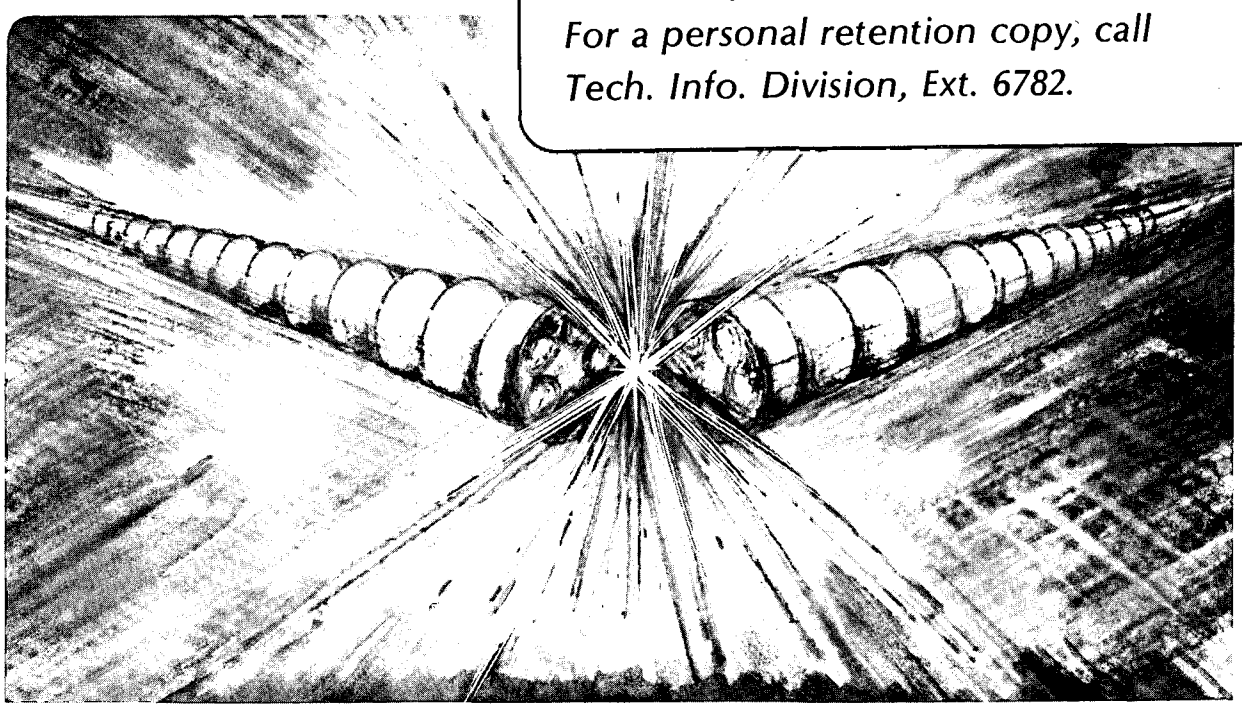

LBL-16832 c.2

Prepared for the U.S. Department of Energy under Contract DE-AC03-76SF00098

DISCLAIMER

This document was prepared as an account of work sponsored by the United States Government. While this document is believed to contain correct information, neither the United States Government nor any agency thereof, nor the Regents of the University of California, nor any of their employees, makes any warranty, express or implied, or assumes any legal responsibility for the accuracy, completeness, or usefulness of any information, apparatus, product, or process disclosed, or represents that its use would not infringe privately owned rights. Reference herein to any specific commercial product, process, or service by its trade name, trademark, manufacturer, or otherwise, does not necessarily constitute or imply its endorsement, recommendation, or favoring by the United States Government or any agency thereof, or the Regents of the University of California. The views and opinions of authors expressed herein do not necessarily state or reflect those of the United States Government or any agency thereof or the Regents of the University of California.

LBL-16832

ION SOURCE OPERATION WITH DIFFERENT MAGNETIC CONFINEMENT GEOMETRIES*

K. N. Leung and K. W. Ehlers

Lawrence Berkeley Laboratory
University of California
Berkeley, California 94720

ABSTRACT

A comparison has been made between the longitudinal line-cusp and the "continuous" checkerboard magnet geometries. We find that the checkerboard arrangement can provide a larger uniform density profile with approximately 20% less plasma density than the longitudinal line-cusp. Results seem to indicate that the reduction in plasma density is closely related to the containment of primary ionizing electrons by the permanent magnets. A new magneto-electrostatic containment scheme was generated by using an internal magnetic cage system. The overall efficiency of this ion source was increased when it was operated with a xenon or argon plasma.

---

*This work was supported by the Director, Office of Energy Research, Office of Fusion Energy, Development and Technology Division, of the U.S. Department of Energy under Contract No. DE-AC03-76SF00098.

INTRODUCTION

It has been shown that permanent magnets can be used to improve the density and uniformity of DC discharge plasmas.[1] Confinement of plasma by different magnet geometries has also been investigated.[2] It was established that the original "broken" checkerboard arrangement adopted by Limpaecher and MacKenzie was less efficient than either the broken or the full-line cusp configuration. In recent years, there has been a growing interest in applying such plasma generators to ion sources for neutral beam injection systems. In the design of these multicusp ion sources, one can encounter poor plasma uniformity at the extraction plane which can be caused by the presence of an axial B-field in the ring-cusp geometry[3] or by the $\vec{E} \times \vec{B}$ drift motion of the charged particles in the longitudinal cusp configuration.[4] In this paper, a comparison has been made between the longitudinal line-cusp and the "continuous" checkerboard geometries. It is found that the checkerboard arrangement can provide a large uniform density profile, but the plasma density at the center of the source is about 20% lower than the longitudinal line-cusp. However when one combines plasma density times the useful ion extraction area, the source efficiency for the checkerboard configuration is still 80% better than the longitudinal line-cusp.

When the multicusp source is operated with plasmas such as argon or xenon, there can be a substantial ion loss to areas in between the line cusps. We have reduced this ion leakage by installing strip-electrodes between the magnet columns.[5] When these electrodes are biased positive relative to the plasma potential, they reflect the positive ions back to

the plasma volume, resulting in an increase of plasma density. An attempt has been made to generate this magneto-electrostatic containment scheme by enclosing the samarium-cobalt magnets in stainless-steel pipes. Since the canned magnets are electrically isolated from the chamber wall, a bias potential can be applied between the wall and the magnet pipes. Experimental results show that a similar increase in xenon or argon plasma density can be obtained when the whole chamber wall is biased positive with respect to the magnets when they are arranged in the line-cusp geometry.

I. EXPERIMENTAL APPARATUS

The experiment was performed in a 2.8 liter stainless-steel chamber (20 cm diam by 24 cm long) with the open end enclosed by a three-grid ion extraction system. The first, or plasma grid, was masked down to a small (0.15×1.3 cm^2) extraction slot in order to reduce the gas loading and the current drawn by the high voltage power supply. The source chamber was surrounded externally by ten columns of samarium-cobalt magnets ($B_{max} \approx 3.6$ kG). These magnets could be arranged to form line-cusps parallel to the source axis with the north and south poles alternately facing the plasma (Fig. 1(a)), or form "continuous" checkerboard geometry as illustrated in Fig. 1(b). In both geometries, the magnet columns on the chamber wall were connected at the end flange by four extras rows of magnets arranged in the line-cusp configuration. Primary electrons were emitted from four 0.05-cm-diam tungsten filaments and the entire chamber wall served as the anode for the discharge.

During normal operation, the hydrogen or argon pressure outside the source was maintained at 1×10^{-4} Torr a measured by an ionization gauge. The actual pressure inside the source was approximately an order of magnitude higher. Plasma parameters and the density profiles were obtained with movable Langmuir probes.

To extract positive ions, the source chamber was biased at approximately +300 V relative to ground potential. The plasma grid was left floating electrically and the second and third grids were both connected to ground. A compact magnetic-deflection spectrometer[6] located just downstream from the extractor was used to measure the hydrogen ion species distribution of the small extracted beam.

In order to install the permanent magnets inside the source chamber, a separate cage structure was fabricated. Eight columns of samarium-cobalt magnets were enclosed inside rectangular stainless-steel pipes (cross-section = 2.2×2.2 cm^2) to generate a line-cusp geometry as illustrated in Fig. 1(c). The pipes were water-cooled and were electrically isolated from the chamber. Thus, a bias potential could be applied between the chamber wall and the canned magnet cage.

II. EXPERIMENTAL RESULTS

A. Comparison of two magnet configurations

The source was first operated with the longitudinal line-cusp configuration as shown in Fig. 1(a). The density and potential of the plasma and the electron temperature were measured both for a hydrogen and an argon plasma. The results are summarized in Table I for a discharge current of 10 A and a discharge voltage of 80 V.

The samarium-cobalt magnets in each column were then rearranged to form a "continuous" checkerboard geometry as illustrated in Fig. 1(b). However, the magnetic field component B_θ measured in between two columns varies from one checkerboard geometry to another (Fig. 2). If the checkerboard is formed by alternating every other magnet (each magnet is 2.54 cm long) in the column (geometry (C) in Fig. 2), the maximum B-field obtained is only 80 gauss. But if one alternates every other pair of magnets (geometry (B) in Fig. 2), then the maximum field is increased to about 270 gauss. If the checkerboard is formed by reversing every three or more magnets in each column, then the B-field will eventually approach that of the line-cusp geometry (A) in Fig. 2. Since the B-field of the checkerboard geometry (C) is too weak for plasma containment, the experimental measurement was made only for checkerboard geometry (B) where every 2 magnets were reversed.

Table I shows the plasma parameters obtained with this checkerboard geometry for both hydrogen and argon plasmas with a discharge current of 10 A and a discharge voltage of 80 V. For both gases, the plasma density for the checkerboard is about 20% lower than that of the line-cusp configuration. The plasma potential V_p is slightly more positive for the checkerboard geometry, indicating that electrons can escape with greater ease. The electron temperature T_e is about the same for both magnet configurations.

In order to understand the difference in plasma density between these two magnet configurations, it is necessary to compare the primary electron density n_p when the source is operated with the same discharge current and background pressure. In the multicusp plasma device, the

primary electrons have an isotropic shell-like distribution.[7] If the neutral pressure is sufficiently low, the primary electron density can be determined from the slope of the straight portion of the Langmuir trace.[8] This technique was used to measure the primary electron densities for the two magnet geometries at a pressure of approximately 8×10^{-6} Torr. In this measurement, the plasma grid was connected to the negative cathode potential so as to reflect the primaries. It was found that n_p in the checkerboard geometry was about 20% lower than that of the line-cusp for the same discharge current and voltage.

Since both the plasma and primary electron densities show the same percentage drop when the line-cusp is converted to the checkerboard configuration, one can conclude that the reduction in plasma density is closely related to the decrease in production rate of plasma per unit volume. On the other hand, the decrease in primary electron density when the checkerboard geometry is used may be due to an increase in the volume occupied by the primaries (because the B-field in between magnet column is weaker) or due to a higher primary electron loss rate (because of a larger anode loss area).

Figure 3 is a plot of the axial plasma density profiles obtained by collecting ion saturation current with a movable Langmuir probe located in between two magnet columns. In the line-cusp configuration, the uniform density profile starts to break off at 6 cm from the side wall, but the uniform region in the checkerboard extends to 4 cm from the wall. Thus, the primaries in the checkerboard occupy a larger volume in the region between the magnet columns. The primaries in this checkerboard arrangement are reflected by the "bridging" B-field in part

of the area above the magnet pole faces. In the case of the line-cusp geometry, the primaries are able to reach the area along the pole face of the magnets. For this reason, it is difficult to estimate the exact difference in the containment volume for the primaries between these two magnet configurations. Nevertheless, by employing the checkerboard configuration, the useful ion extraction area for this source is increased by a factor of 2.26. Even though the plasma density in this magnet geometry drops by 20%, the overall efficiency of the ion source is still increased by 80%.

The "effective" anode area for these two magnet configurations is best illustrated by the erosion pattern developed on the source chamber wall as shown in Fig. 4. The straight white lines in the picture show approximately the loss area of the primaries along the line cusps while the four corner "stars" indicate the loss area when the checkerboard geometry is used. The picture seems to show that the effective anode area for the checkerboard is <u>larger</u> than that of the line-cusp.

The hydrogen ion species distribution for the two magnet geometries has also been determined by extracting a small low energy beam from the source. Figure 5(a) shows a plot of the species distribution as a function of the discharge current I_a. For the range of I_a considered, the H_3^+ ion fraction is always higher for the checkerboard, while the H_2^+ and H^+ ion concentrations are lower. Since the primary electron density is higher in the line-cusp configuration, one would expect that a larger number of H_3^+ ions are being dissociated according to the reaction[9] $e + H_3^+ \rightarrow 2H + H^+ + e$. As a result, one should find a lower H_3^+ concentration for this magnet configuration.

The presence of energetic electrons in the neighborhood of the extractor can easily generate H_2^+ ions which are then extracted immediately from the source.[10] The plasma grid in the line-cusp geometry always floats at a potential lower than that of the checkerboard (Fig. 5(b)). This result indicates that more energetic electrons arrive at the extractor for this magnet geometry. Hence, the H_2^+ ion percentage in the extracted beam should be higher. The combined effect of these two processes will result in a slightly higher H^+ ion fraction for the line-cusp configuration.

B. Internal magnet cage system

When the permanent magnets are arranged in the line-cusp configuration, the loss of plasma to areas between cusps can be substantial if the source is operated with massive ions such as argon or xenon. In a previous experiment,[5] we have succeeded in reducing this ion leakage by installing strip-electrodes in between magnet columns. When these electrodes are biased positively with respect to the anode, they reflect the positive ions back to the plasma volume, resulting in an increase of plasma density.

An attempt has been made to generate this magneto-electrostatic plasma containment scheme by using an internal magnet cage structure. The samarium-cobalt magnets, arranged in the line-cusp configuration, were canned inside rectangular stainless-steel pipes as illustrated in Fig. 6. A cross-sectional view of the source chamber with the magnet cage is shown in Fig. 7. The pipes now form the main anode for the discharge. They are water-cooled and are electrically isolated from the

source chamber wall. A separate power supply is used to bias the entire chamber wall at a potential more positive or negative with respect to the stainless-steel pipes.

When the source is operated with a hydgrogen plasma, the Langmuir probe traces (a, b and c) in Fig. 8(a) show no significant difference in the plasma density when the chamber wall is either floating, biased at the same potential, or at +10 V with respect to the magnet cage. This result demonstrates that the B-field in the region between cusps is sufficiently strong to contain most of the hydrogen ions. Consequently, the maximum current drawn by the bias power supply (Fig. 9(a)) is also very small.

When argon gas is used for the discharge, the probe traces (a and b) in Fig. 8(b) show that there is no significant change in plasma density whether the chamber wall is floating or biased at anode potential. But when the chamber wall is biased at +10 V, the plasma density (as illustrated by the probe trace b) increases by about 18%. This gain in plasma density requires only 7% more power supplied to the system (Fig. 9(b)). The plasma potential V_p increases by 1.5 V but is 3.5 V more negative than the wall potential. Hence the argon ions are now contained electrostatically in the region between cusps.

When the more massive gas xenon is used, the probe traces (a and b) in Fig. 8(c) show that the density increases by 33% as the wall bias voltage is varied from 0 to +10 V. But the extra power consumed by the system increases only by 13% (Fig. 9(c)). The increase in V_p (~4 V) indicates that the confinement of the positive ions has been improved. When the wall is floating electrically, probe trace c in Fig. 8(C) shows

the density decreases by 11% and V_p becomes approximately 0.4 V more negative than the case when the wall is at the same potential as the magnet cage. Biasing the wall more negative will therefore enhance the loss rate of the xenon ions.

The use of this internal magnet cage system allows one to construct the source chamber with the proper thickness (against vacuum) without serious attenuation of the cusp fields. This magnetoelectrostatic containment scheme involves no geometric perturbation to the plasma and should make the multicusp source useful for the generation of the heavy ions used for plasma etching, ion machining, or ion implantation purposes. In fact, we have applied this technique in the construction of a new self-extraction negative ion source which will be operated with cesium.

ACKNOWLEDGMENTS

We would like to thank D. Moussa and C. A. Matuk for technical assistance. This work is supported by the Director, Office of Energy Research, Office of Fusion Energy, Development and Technology Division, of the U. S. Department of Energy under Contract No. DE-AC03-76SF00098.

REFERENCES

1. R. Limpaecher and K. R. MacKenzie, Rev. Sci. Instrum. 44, 726 (1973).
2. K. N. Leung, T. K. Samec, and A. Lamm, Phys. Lett. A51, 490 (1975).
3. K. W. Ehlers and K. N. Leung, Rev. Sci. Instrum. 52, 1452 (1981).
4. K. W. Ehlers and K. N. Leung, Rev. Sci. Instrum. 50, 1353 (1979).
5. K. W. Ehlers and K. N. Leung, Rev. Sci. Instrum 53, 1429 (1982).
6. K. W. Ehlers, K. N. Leung and M. D. Williams, Rev. Sci. Instrum. 50, 1031 (1979).
7. T. Samec and R. Stenzel, Bull. Am. Phys. Soc. 17, 1917 (1972).
8. K. N. Leung, Noah Hershkowitz and K. R. MacKenzie, Phys. Fluids, 19, 1045 (1976).
9. B. Peart and K. T. Dolder, J. Phys. B 8, L143 (1975).
10. K. W. Ehlers and K. N. Leung, Rev. Sci. Instrum. 52, 1452 (1981).

FIGURE CAPTIONS

Fig. 1 Schematic diagram of the ion source showing; (a) the longitudinal line-cusp, (b) the checkerboard, and (c) the internal magnet cage arrangement.

Fig. 2 A plot of the magnetic field component B_θ, measured between two center magnet rows on the end flange, as a function of the axial position for three different magnet configurations. The dots on the upper right hand corner of the diagram indicate where the measurements are taken.

Fig. 3 Radial plasma density profiles for the checkerboard and line-cusp magnet configurations.

Fig. 4 Erosion pattern generated on the chamber wall after the source has been operated with the line-cusp and checkerboard geometries.

Fig. 5 (a) Hydgrogen ion species distribution, and (b) plasma grid floating potential as a function of discharge current for the line-cusp (solid lines) and checkerboard (dotted lines) magnet arrangements.

Fig. 6 The canned magnet cage structure in the source chamber and on the end flange.

Fig. 7 Cross-sectional view of the source chamber together with the internal magnet cage.

Fig. 8 Langmuir probe characteristics obtained with the chamber wall biased at anode potential (indicate by a), at +10 V relative to the anode (indicate by b), and floating electrically (indicate by c) for three different types of plasmas.

Fig. 9 The V-I characteristics of the bias power supply when the source is operated with hydrogen, argon and xenon plasmas.

Table 1. Plasma parameters obtained for two different magnet geometries with discharge voltage = 80 V and discharge current = 10 A.

Gas	Magnet geometry	V_p (V)	T_e (eV)	n (ions/c.c.)
Hydrogen	line-cusp	+3.3	2.7	3.6×10^{11}
	checkerboard	+3.7	2.5	2.9×10^{11}
Argon	line-cusp	+4.6	2.9	5.7×10^{11}
	checkerboard	+5.5	2.9	4.6×10^{11}

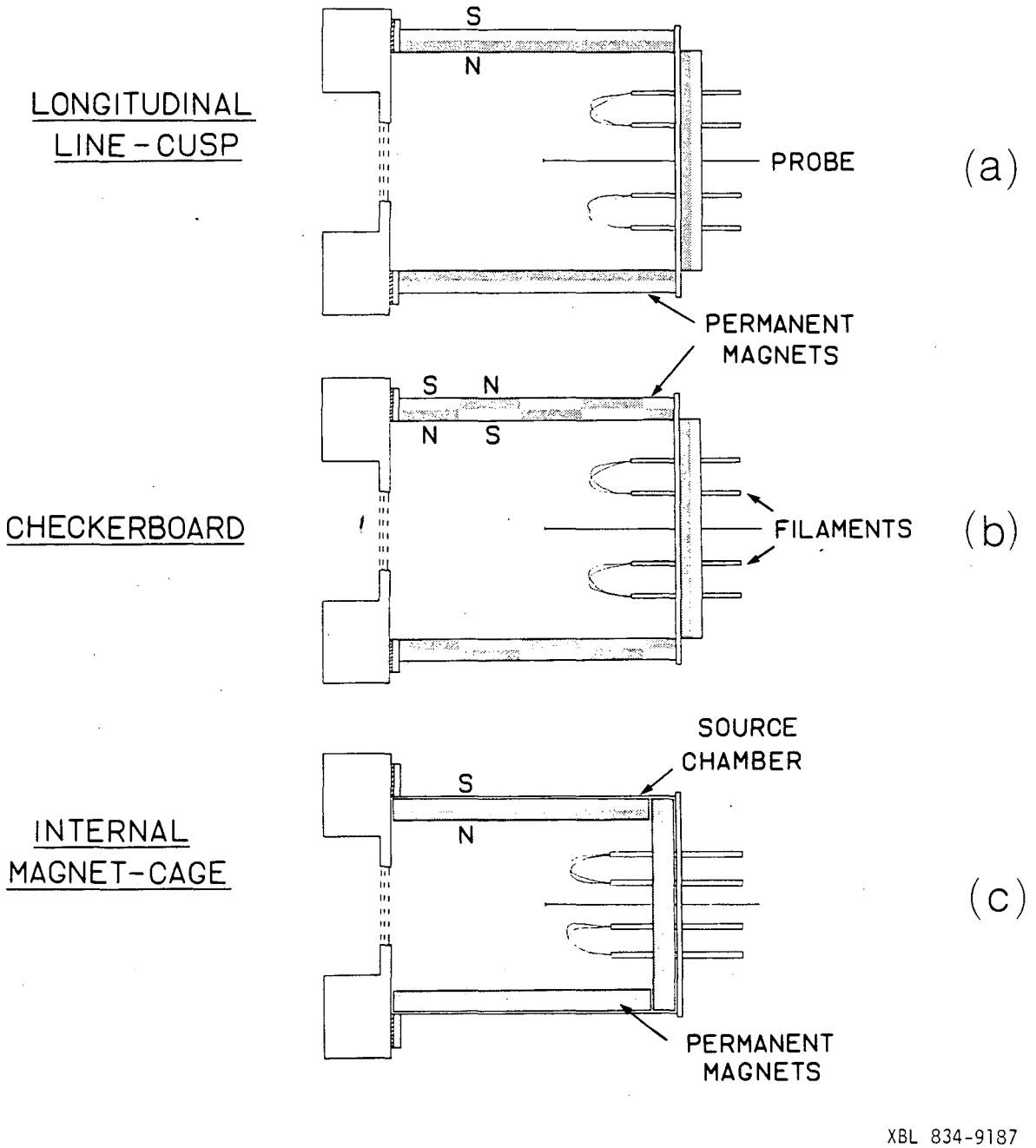
LONGITUDINAL
LINE-CUSP
S
N
PROBE
(a)
PERMANENT
MAGNETS
CHECKERBOARD
S N
N S
FILAMENTS
(b)
SOURCE
CHAMBER
INTERNAL
MAGNET-CAGE
S
N
(c)
PERMANENT
MAGNETS
XBL 834-9187

Fig. 1

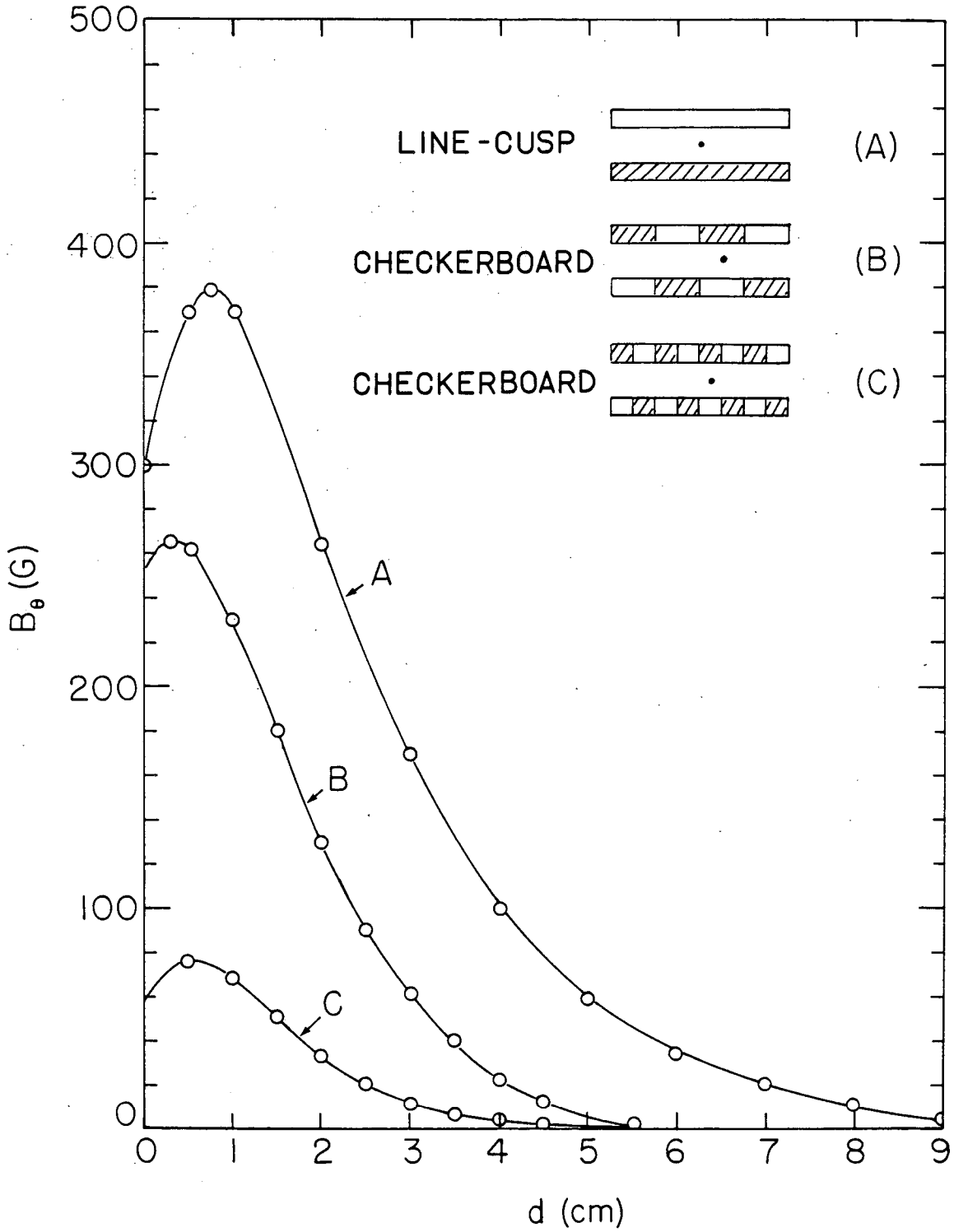

XBL 835-9786

Fig. 2

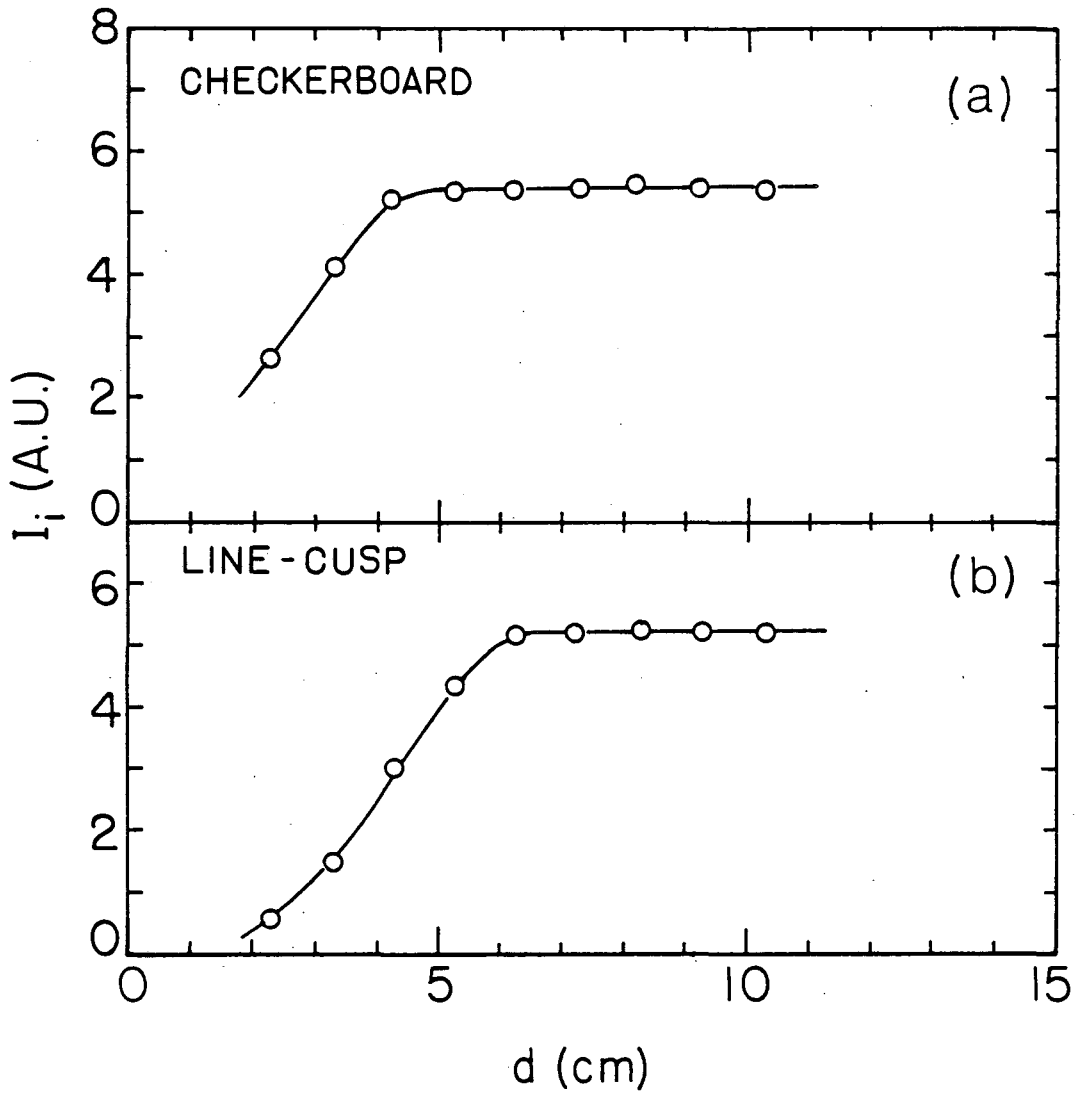

XBL 835-9784

Fig. 3

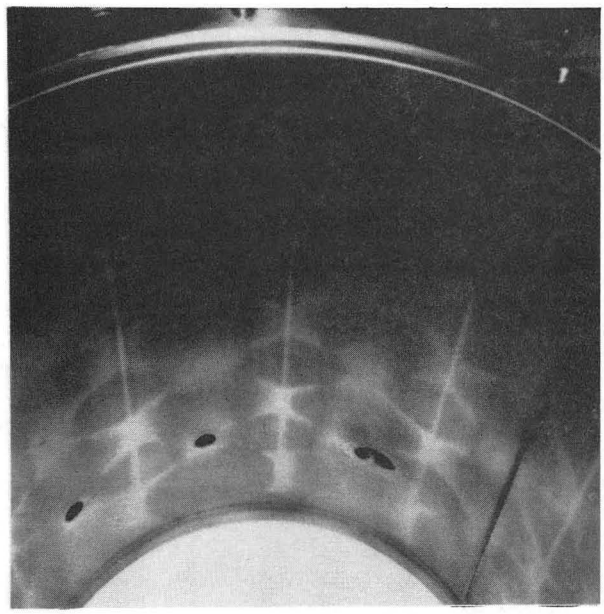

CBB 836-5366

Fig. 4

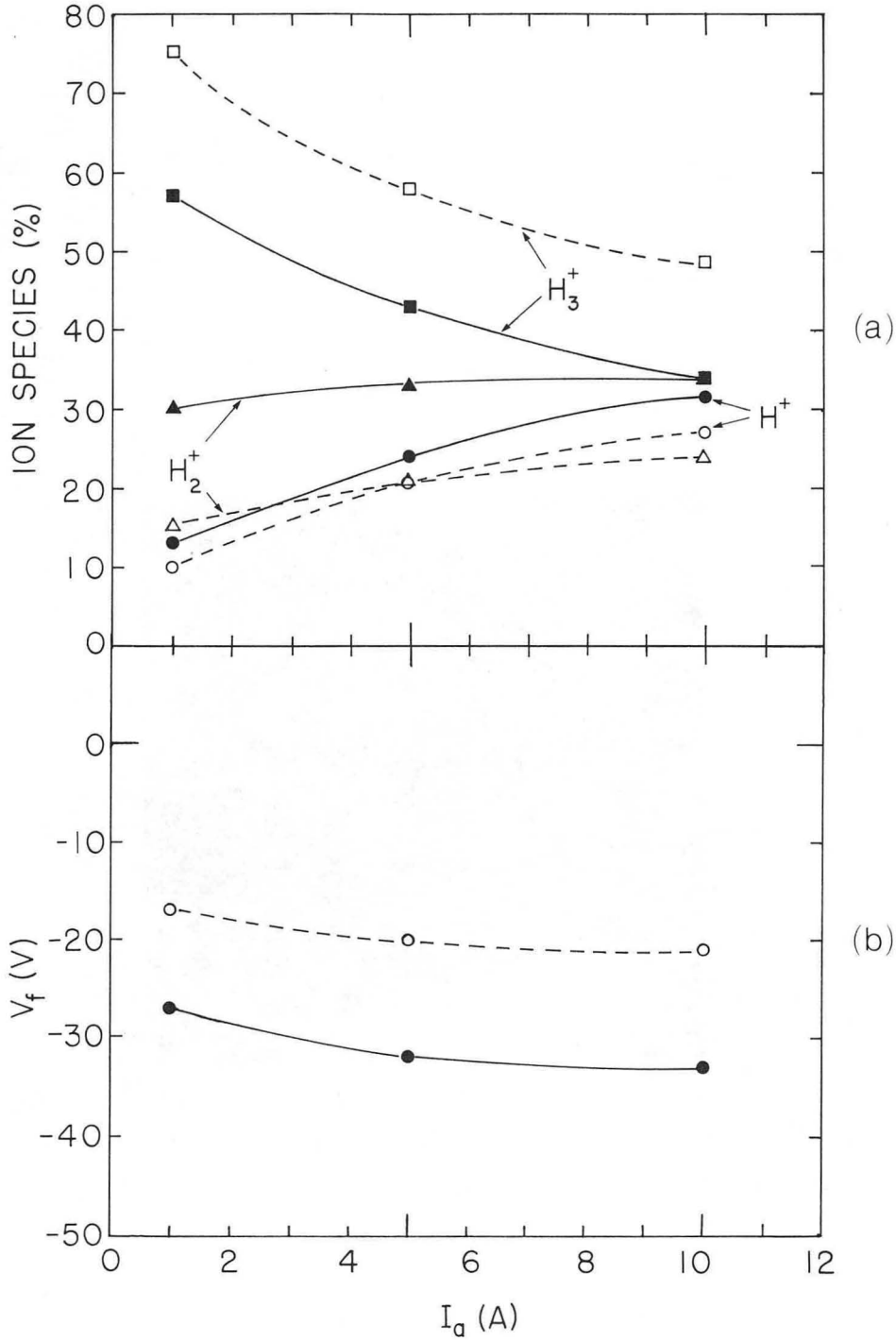

XBL 835-9787

Fig. 5

THE INTERNAL MAGNET CAGE STRUCTURE

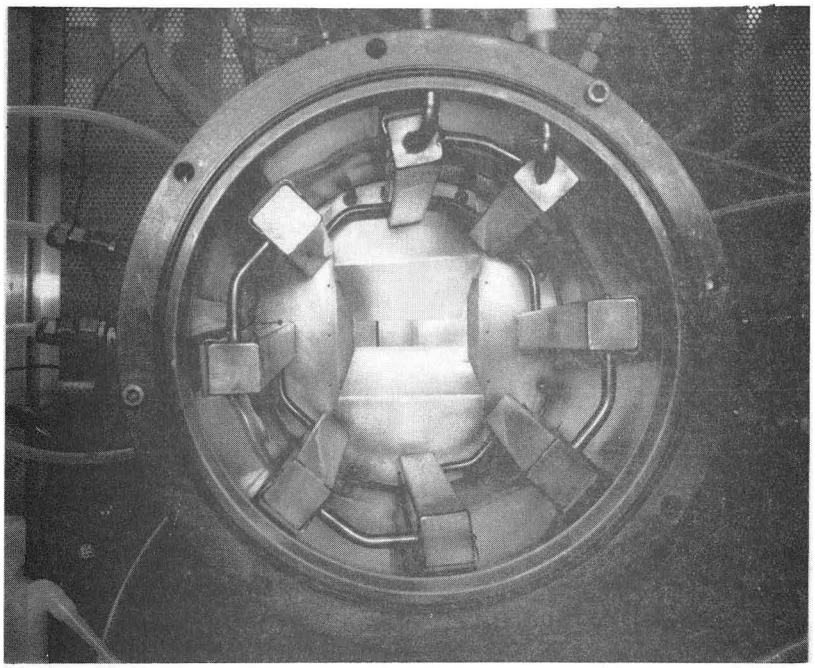

(a)

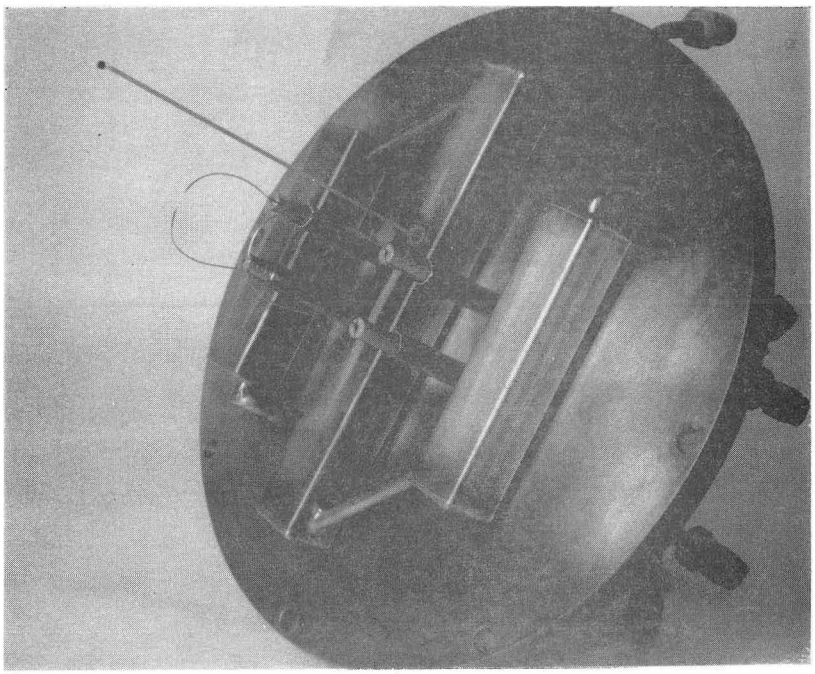

(b)

XBB 8310-9578

Fig. 6

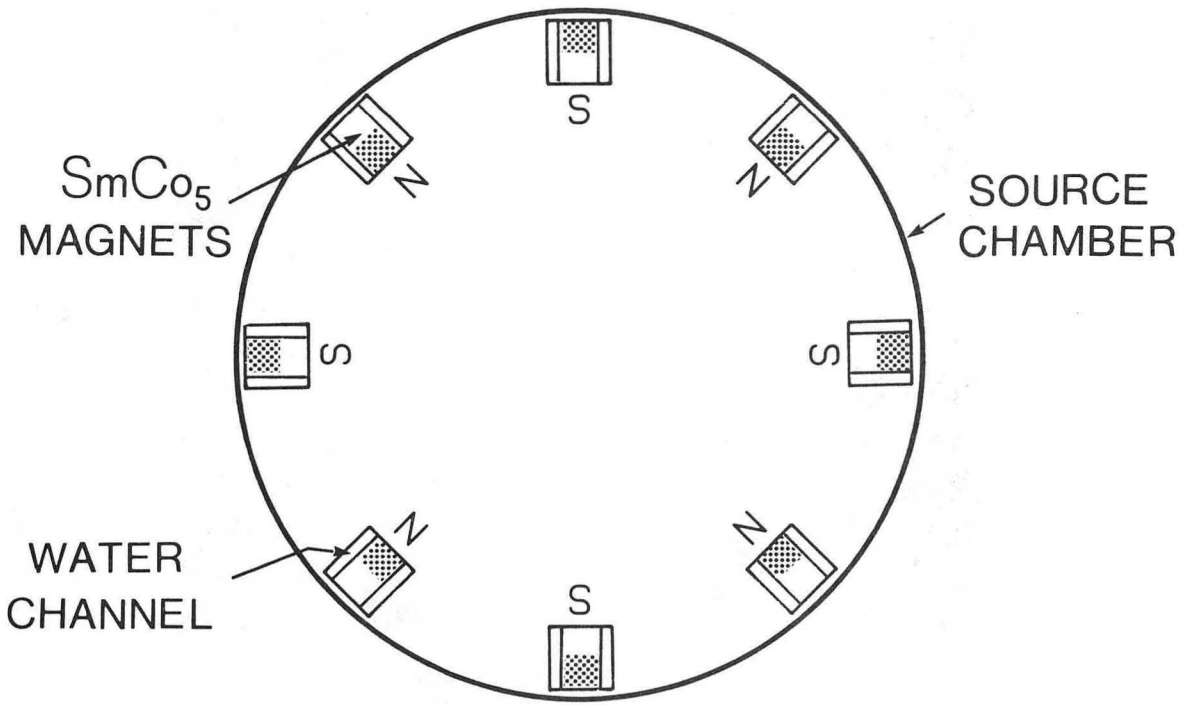

XBL 834-9186

Fig. 7

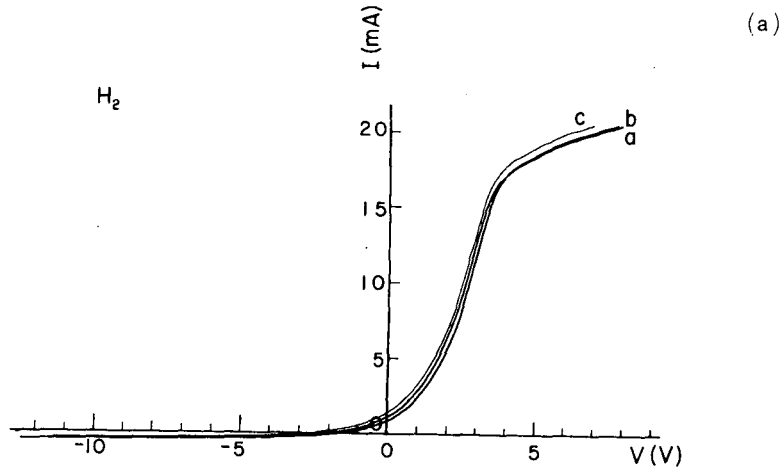

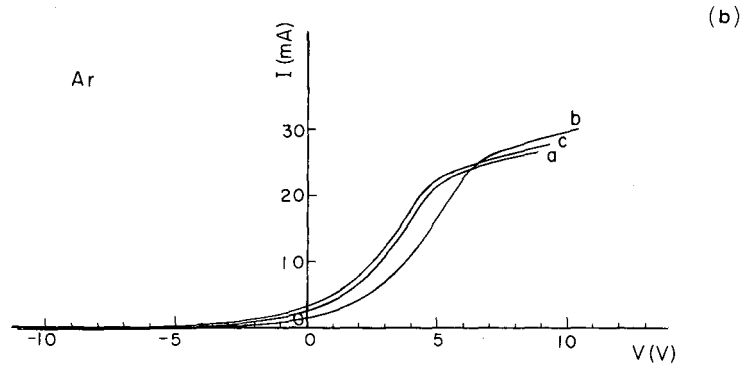

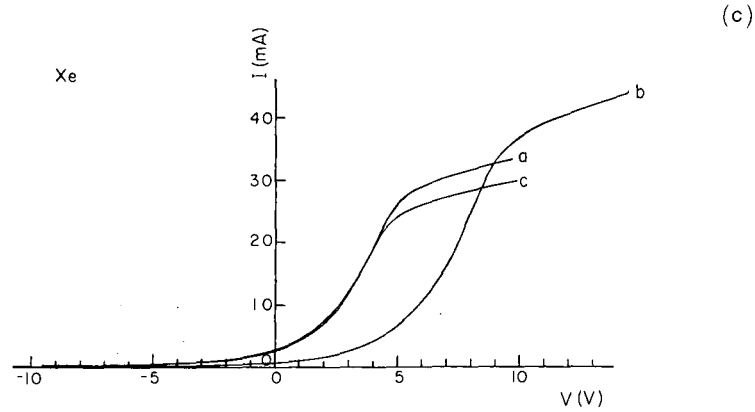

XBL 835-9782A

Fig. 8

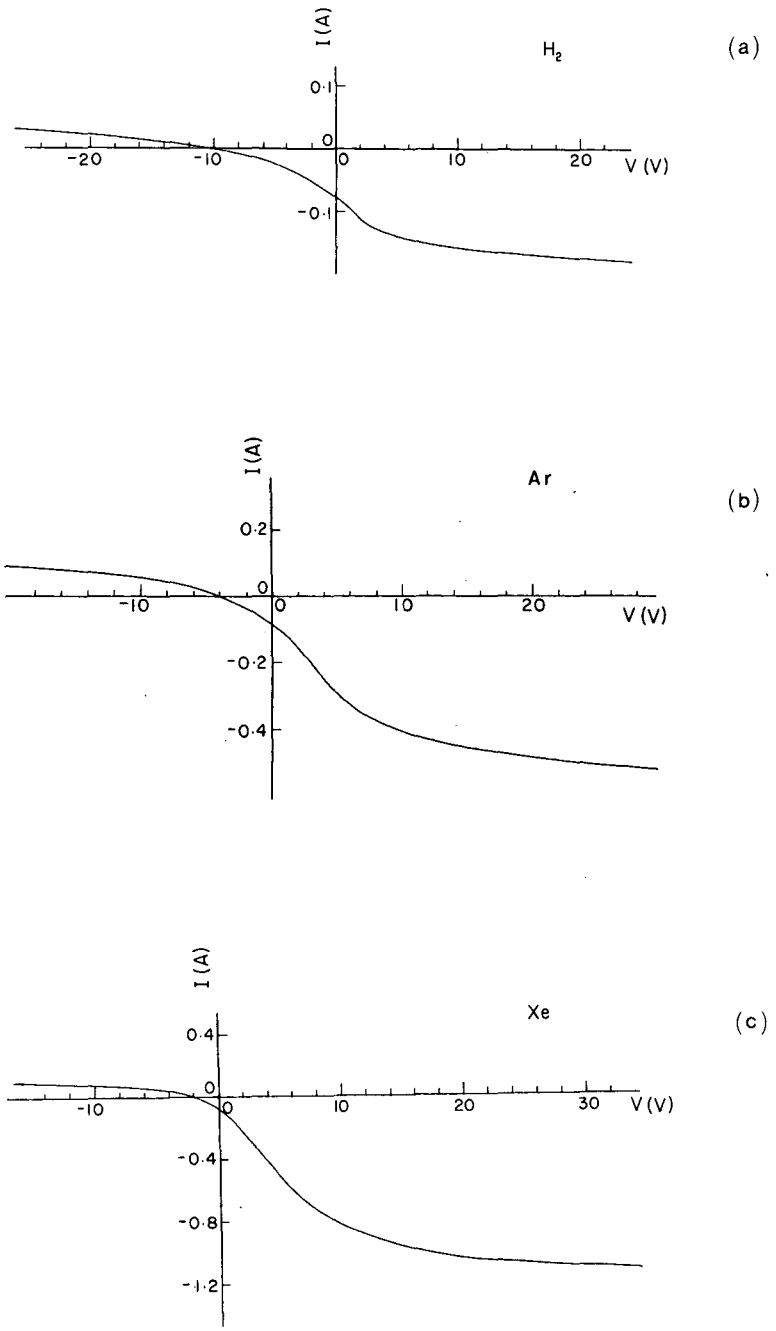

XBL 836-10190

Fig. 9

This report was done with support from the Department of Energy. Any conclusions or opinions expressed in this report represent solely those of the author(s) and not necessarily those of The Regents of the University of California, the Lawrence Berkeley Laboratory or the Department of Energy.

Reference to a company or product name does not imply approval or recommendation of the product by the University of California or the U.S. Department of Energy to the exclusion of others that may be suitable.

TECHNICAL INFORMATION DEPARTMENT
LAWRENCE BERKELEY LABORATORY
UNIVERSITY OF CALIFORNIA
BERKELEY, CALIFORNIA 94720